Cyclic(Alkyl)(Amino) Carbene-Promoted Ring Expansion of a Carbodicarbene Beryllacycle

Jacob E. Walley,[†] Akachukwu D. Obi,[†] Grace Breiner,[†] Guocang Wang,[†] Diane A. Dickie,[†] Andrew Molino,[‡] Jason L. Dutton,[‡] David J. D. Wilson,[‡] Robert J. Gilliard, Jr.[†*]*

[†]Department of Chemistry, University of Virginia, 409 McCormick Rd, PO Box 400319, Charlottesville, USA

[‡]Department of Chemistry and Physics, La Trobe Institute for Molecular Science, La Trobe University, Melbourne, Australia.

Abstract

Recent synthetic efforts have uncovered several bond activation pathways mediated by beryllium. Having the highest charge density and electronegativity, the chemistry of beryllium often diverges from that of its heavier alkaline earth metal congeners. Herein, we report the synthesis of a new carbodicarbene beryllacycle (**2**). Compound **2** converts to **3** via an unprecedented cyclic(alkyl)(amino) carbene (CAAC)-promoted ring expansion reaction (RER). While CAAC activates a carbon–beryllium bond, N-heterocyclic carbene (NHC) coordinates to beryllium to give the tetracoordinate complex **4** which contain the longest ^{carbene}C–Be bond to date at 1.856(4) Å. All of the compounds were fully characterized by X-ray crystallography, FT-IR, ^{1}H, ^{13}C, and ^{9}Be NMR. The ring expansion mechanism was modeled with both NHC and CAAC using DFT

calculations. While, the activation energy for the observed beryllium ring expansion with CAAC was found to be 14 kJ mol^{-1}, the energy barrier for hypothetical NHC RER is significantly higher (199.1 KJ mol^{-1}).

Introduction

The chemistry of beryllium has witnessed a resurgence of interest due in part to discoveries in subvalent and hydridic beryllium compounds.[1-5] Many of these highly reactive beryllium species have been stabilized by neutral singlet carbenes,[5] which are divalent carbon-based ligands that are σ-donating (HOMO) and π-accepting (LUMO) in character.[6-7] The first stable carbene, a (phosphino)(silyl)carbene, was discovered by Bertrand in 1988.[8] Nearly three years later, Arduengo structurally characterized the first stable *N*-heterocyclic carbene (NHC).[9] In comparison to NHCs, cyclic(alkyl)(amino) carbenes (CAAC), reported by Bertrand in 2005, show enhanced σ-donor and π-acceptor properties.[10] Hill prepared the first structurally characterized organoberyllium hydrides supported by NHCs, $[(NHC)Be(CH_3)H]_2$.[3-4] Interestingly, the reaction of this dimeric complex with phenylsilane results in beryllium insertion into a C–N bond to produce a six-membered beryllacycle (Figure 1A). Braunschweig isolated the first molecular beryllium(0) complex, $Be(^{R2}CAAC)_2$ [R = CH_3, or Cy], by reducing $(^{Me2}CAAC)BeCl_2$ with two equivalents of potassium graphite (KC_8) in the presence of free ^{R2}CAAC (Figure 1B).[1] Our laboratory recently synthesized $[Be(^{Et2}CAAC)_2]$ and demonstrated the utility of these subvalent compounds as reducing agents and ligand transfer agents.[2] This ultimately led to the isolation of the first carbene–bismuthinidene, which could not be isolated by traditional reduction strategies (Figure 1C).[2]

Carbodicarbenes (CDC), a class of carbon(0) ligands categorized as carbones, were theorized in 2007 by Frenking[11] and isolated by Bertrand[12] in 2008. Since then, Ong has developed new synthetic pathways that have diversified the library of CDCs, which include symmetric[13] and unsymmetric[14] analogues. CDCs are exceptionally stronger σ-donors than NHCs and CAACs, and are π-donating instead of π-accepting.[15] Owing to their unique electronic properties CDCs have been shown to activate small molecules *via* a 1,2-addition reaction,[16] however, NHCs and CAACs proceed by 1,1 addition pathways.[17-21] While the coordination chemistry of NHCs and CAACs to main group elements is well known,[6, 22-24] there are only a handful of reports which employ carbones.[25-29] Due to our group's interest in studying the coordination chemistry of alkaline earth metals and their potential to activate chemical bonds,[29-31] we recently synthesized the first examples of CDC s-block complexes and demonstrated that a heteroleptic (CDC)BeCl[$N(SiMe_3)_2$] complex undergoes a formal C–H bond activation to form a five-membered beryllacycle (Figure 1D).[29] While several examples exist for five-[3, 29, 32-34] and six-[3, 34-39] membered N-containing beryllacycles, there are currently no examples of ring expansion reactions involving beryllium rings.

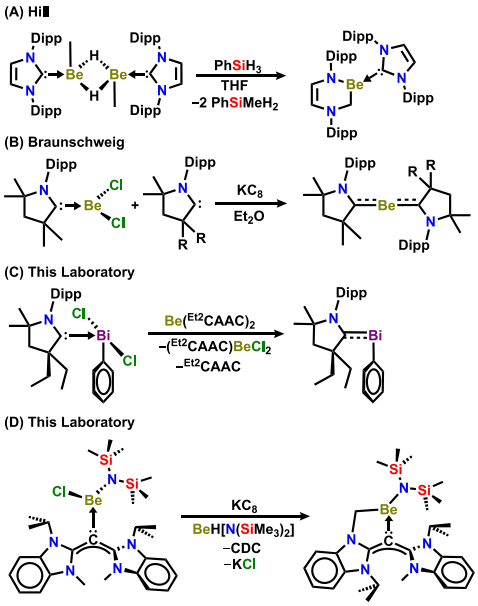

Figure 1. (A) Beryllium-mediated C–N bond activation and ring expansion; (B) Synthesis of molecular beryllium(0) complexes (R = methyl or cyclohexyl); (C) Beryllium(0) as a reducing agent for the synthesis of the first carbene-bismuthinidene; (D) C–H activation and cyclization at a beryllium center.

Herein, we report the synthesis, molecular structure, and computations of a new five-membered beryllacycle (**2**). Compound **2** undergoes an unprecedented CAAC-mediated ring expansion reaction to yield the six-membered beryllacycle **3**. While diamidocarbenes have been shown to facilitate the Büchner ring expansion of arenes,[40] this is the first example of CAAC promoting a ring expansion reaction *via* activation of a Be–C bond. This behavior is in contrast to that of an NHC ligand, sIPr (sIPr = 4,5-dimethyl-1,3-diisopropylimidazolin-2-ylidene), which readily coordinated to the beryllium center in **2** to form the tetrahedral compound **4**.

Results and Discussion

Synthesis and Reactivity of Carbodicarbene Beryllacycle

Scheme 1. Beryllacycle Anion Exchange Reaction.

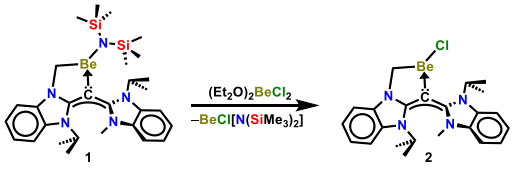

NHC and CAAC do not react with compound **1** due to the larger steric bulk, therefore a solution of compound **1** in a toluene/hexane mixture was treated with beryllium dichloride dietherate, $(Et_2O)_2BeCl_2$, and allowed to stir. This metathesis reaction formed $BeCl[N(SiMe_3)_2]$,[41] which was confirmed by ^{9}Be NMR (Figure S10). After two days, compound **2** was isolated as a yellow solid in 76% yield. The ^{1}H NMR in C_6D_6 showed two heptets at 5.58 ppm and 3.31 ppm, which were shifted slightly from the starting material **1** (5.57 ppm and 3.36 ppm).[29] Interestingly, the two doublets (2.84 ppm and 2.79 ppm) attributed to the diastereotopic methylene protons on the carbon atom adjacent to beryllium were shifted downfield from **1** (2.75 ppm and 2.60 ppm) and had merged significantly (Figure S1).[29] This can be explained by the less sterically demanding chloride allowing for facile rotation of the N-heterocyclic carbene (NHC) moiety in compound **2** with respect to **1**, which is hindered by the bulky $[N(SiMe_3)_2]^-$ group. The ^{13}C NMR showed a singlet at 164.9 ppm which was attributed to the carbone carbon. This is consistent with our previously reported CDC beryllium complexes (160.3-164.4 ppm).[29]

Yellow block-shaped crystals of compound **2** suitable for X-ray diffraction were obtained from a toluene/hexane mixture at –37 °C (Figure 2). The beryllium atom resides in a distorted trigonal planar environment with two carbon–beryllium bonds [Be1–C3: 1.769(3) Å and Be1–C1: 1.743(3) Å] and one beryllium–chloride bond [Be1–Cl1: 1.916(2) Å]. The C1–Be1 bond in **2** [1.743(3) Å]

is significantly shorter than that in **1** [1.796(5) Å] suggesting a stronger ^{carbone}C–Be interaction for **2**. In support of this greater electronic contribution from the carbone to the beryllium, the C1–C2 bond distance in **2** [1.391(2) Å] is longer than that in **1** [1.373(4) Å].

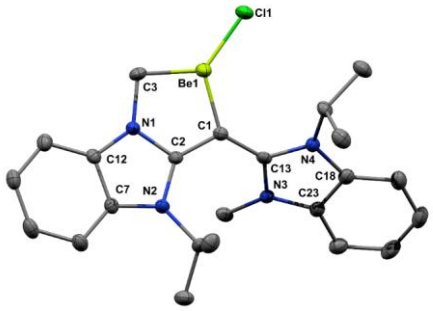

Figure 2. Molecular structure of **2** (thermal ellipsoids at 50% probability; H atoms and non-coordinating solvent omitted for clarity). Selected bond distances (Å) and angles (deg): Be1–Cl1: 1.916(2); Be1–C1: 1.743(3); C1–C2: 1.391(2); C2–N1: 1.378(2); N1–C3: 1.471(2); Be1–C3: 1.769(3); C1–C13: 1.403(2). C1–Be1–C3: 101.01(14); C1–Be1–Cl1: 129.41(14); C3–Be1–Cl1: 129.56(14); C2–C1–C13: 125.28(15) C2–C1–Be1: 103.55(14).

Scheme 2. CAAC-Promoted Ring Expansion and NHC Coordination to Beryllium.

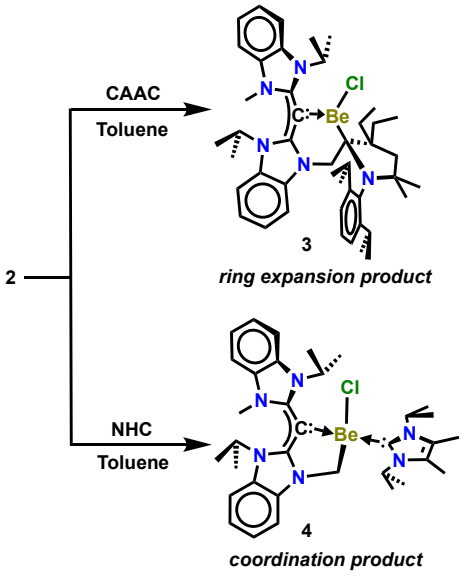

Due to the open coordination site on compound **2**, we were motivated to explore its coordination chemistry with carbenes. In toluene, a solution of ^{Et2}CAAC was added to a stirring suspension of **2**. Immediately upon addition, a yellow product formed in solution. After workup, compound **3** was isolated as a yellow solid in 84% yield. The ^{1}H NMR showed two doublets at 2.98 and 2.25 ppm, attributed to diastereotopic methylene protons of the five-membered CAAC ring. This is in contrast to a singlet at 1.71 ppm for free ^{Et2}CAAC. Interestingly, two heptets at 4.96 and 4.79 ppm for the methine protons of the diisopropylphenyl (Dipp) moiety suggest that the rotation of the Dipp group is hindered by steric crowding.

Yellow rod-shaped crystals of **3** were obtained by slow evaporation of toluene. The structure revealed that the ^{Et2}CAAC carbene carbon (C24) inserted into the Be1–C3 bond of **2** to form a six-membered beryllacycle (Figure 3). The trigonal planar geometry surrounding the beryllium is significantly less distorted than **2** with a C1–Be1–C24 angle of 114.46(17)°, compared to

101.01(14)° for **2** (C1–Be1–C3). The Be1–C1 bond (1.754(3) Å) is longer than that of **2**, indicating less electron donation from ^{carbone}C to Be. While CAAC has been shown to insert into d-block metal–carbon bonds,[42-43] this is the first example where CAAC inserts into an s-block metal–carbon bond.

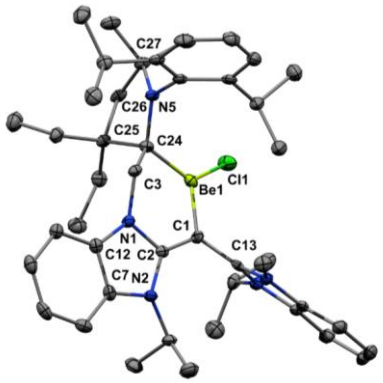

Figure 3. Molecular structure of **3** (thermal ellipsoids at 50% probability; H atoms omitted for clarity). Selected bond distances (Å) and angles (deg): Be1–Cl1: 1.973(3); Be1–C1: 1.754(3); C1–C2: 1.387(3); C2–N1: 1.392(2); N1–C3: 1.467(2); C3–C24: 1.531(3); Be1–C24: 1.791(3); C1–C13: 1.428(3). C1–Be1–C24: 114.46(17); C1–Be1–Cl1: 119.13(16); C24–Be1–Cl1: 126.13(16); C2–C1–C13: 118.63(17); C2–C1–Be1: 115.70(18).

We considered that the carbene insertion into the Be1–C1 bond of compound **2** might be related to the enhanced electrophilicity of ^{Et2}CAAC. Therefore, we reacted **2** with sIPr, a traditional NHC. A solution of sIPr was added to a stirring suspension of **2** in toluene. Immediately upon addition, a yellow product formed in solution. After workup, compound **4** was isolated as a yellow solid in 86% yield. The peaks in the ^{1}H NMR of compound **4** in C_6D_6 were broadened significantly, therefore, the ^{1}H NMR spectrum was obtained in CD_2Cl_2. Two heptets at 5.35 and 3.77 ppm are attributed to the methine protons of the isopropyl groups on the CDC moiety. A heptet at 5.16 ppm

was attributed to the methine protons of the isopropyl groups for a coordinated sIPr ligand. The ^{13}C NMR revealed a peak at 181.5 ppm was attributed to the carbene carbon of the coordinated sIPr, which is comparable to the tetrahedral $[(sIMe)_3BeCl]Cl$ (sIMe = 1,3-dimethylimidazolin-2-ylidene) and $[BeCl_2(I^iPr)_2]$ (I^iPr = 1,3-diisopropylimidazolin-2-ylidene) (174.9 and 176.6 ppm, respectively).[44-45]

Yellow rod-shaped crystals of **4** were obtained by slow evaporation of a toluene/hexane mixture (Figure 4). The structure features a beryllium atom in a distorted tetrahedral geometry, with the C1–Be1–C3 angle (94.65(17)°) being the largest deviation from 109.5°. The ^{carbone}C–Be bond of **4** is 1.862(4) Å, which is significantly longer than those of the beryllacycles **1**-**3**. In support of this significantly elongated ^{carbone}C–Be dative bond, the allenic bond lengths C1–C2 and C1–C13 (1.387(3) Å and 1.373(4) Å, respectively) are in agreement with greater ^{carbone}C to ^{carbene}C π-donation. The Be1–Cl1 bond distance is 2.084(3) Å, which is close to 2.091 Å for $[(sMe)_3BeCl]Cl$.[45] The C24–Be1 bond distance in **4** (1.856(4) Å) is the longest reported ^{carbene}C–Be bond to date, while previously reported ^{carbene}C–Be bonds are within the range of 1.765–1.822 Å.[23]

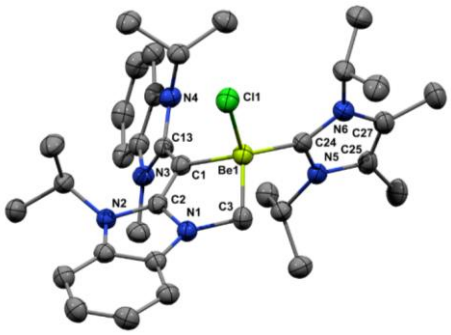

Figure 4. Molecular structure of **4** (thermal ellipsoids at 50% probability; H atoms omitted for clarity). Selected bond distances (Å) and angles (deg): Be1–Cl1: 2.084(3); Be1–C24: 1.856(4);

Be1–C1: 1.862(4); C1–C2: 1.387(3); C2–N1: 1.361(3); N1–C3: 1.474(3); Be1–C3: 1.833(4); C1–C13: 1.373(3). C1–Be1–C3: 94.65(17); C1–Be1–Cl1: 106.38(15); C3–Be1–Cl1: 106.89(16); C3–Be1–C24: 113.08(18); C24–Be1–C1: 118.46(19); C24–Be1–Cl1: 115.07(16); C2–C1–C13: 125.3(2).

Compounds **2**–**4** were also analyzed by infrared spectroscopy (Figures S11–S13). Broad bands representative of the allene asymmetric stretching frequency were observed at 1548 cm^{-1} and 1541 cm^{-1} for compounds **2** and **4**, which is only slightly less than 1552 cm^{-1} for compound **1**.[29] A broad band at 1518 cm^{-1} was assigned to the allene asymmetric stretching mode for compound **3**. This shift to lower wavenumbers is a result of decreased ring strain. It is noteworthy that these trends were reproduced by calculations at the B3LYP-D3(BJ)/def2-TZVP level of theory (Figure S14).

The ^{9}Be NMR data were obtained for the tricoordinate compounds **2** and **3**, as well as the tetracoordinate compound **4**. These gave resonances at 18.2, 14.0, and 5.3 ppm, respectively. The ^{9}Be NMR spectra for compounds **2** and **3** show broad signals, which are consistent with reported tricoordinate beryllium complexes.[1-4, 29, 39, 44] The ^{9}Be NMR signal for compound **4** falls within the range of known tetrahedral beryllium compounds (0.8–5.5 ppm),[39, 44-48] and is notably sharper than the tricoordinate complexes **2** and **3**. This broadening is attributed to the quadripolar coupling effect associated with the anisotropic ^{9}Be nuclei, which is expected to be zero for perfectly symmetric tetrahedral beryllium complexes.[39] Distortion from this ideal geometry or lower coordination numbers results in broadened chemical shifts.

Theoretical Analysis

A theoretical exploration of the mechanism for the ring expansion of **2** with both CAAC (observed) and NHC (unobserved) was carried out. Model NHC and CAAC ligands with N–Me

substituents (labelled ^{Me}NHC and ^{Me}CAAC, Figure 5) were utilized for computational efficiency, which has been demonstrated to yield equivalent results to bulky substituents.[49-50]

The expected difference in reactivity between NHC and CAAC is shown in the reaction energy profile for the ring expansion reaction (RER) of **2** (Figure 5). Initial adduct formation is favorable between **2** and both ^{Me}NHC **4** and ^{Me}CAAC **5** (ΔG = -24.5 and -33.2 kJ mol^{-1}, respectively). However, the barrier for Be–C bond activation with ^{Me}NHC **TS1$_{NHC}$** is 199.1 kJ mol^{-1}, which was inaccessible under the given experimental conditions. Moreover, the ring expanded product with ^{Me}NHC is 58.3 kJ mol^{-1} higher in free energy relative to the free reactants (**2** and ^{Me}NHC). Clearly, RER of **2** by NHC is both kinetically and thermodynamically unfavorable, which is consistent with the lack of observed RER with NHC. In contrast, with ^{Me}CAAC the **TS1$_{CAAC}$** barrier for Be–C bond activation is low (14.0 kJ mol^{-1}), which readily leads to the thermodynamically favorable ring expanded product **3** (-40.9 kJ mol^{-1}). The low barrier is consistent with non-forcing experimental conditions for the reaction to produce **3**.

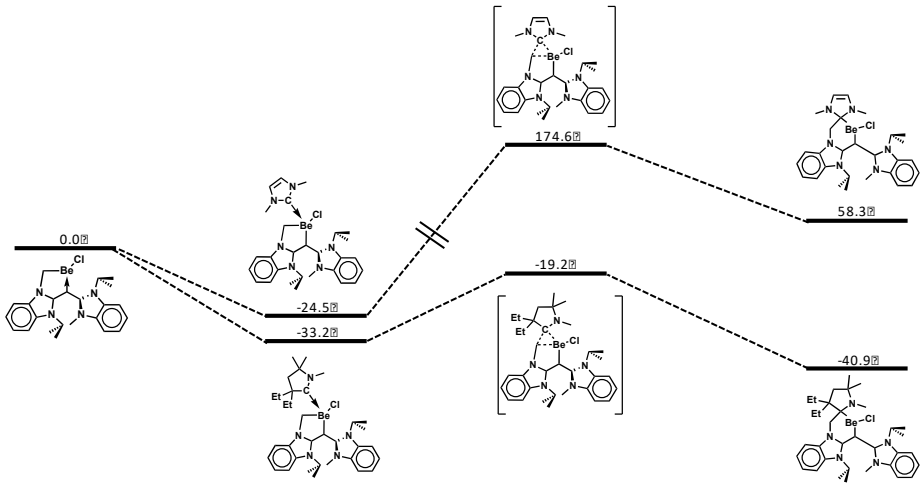

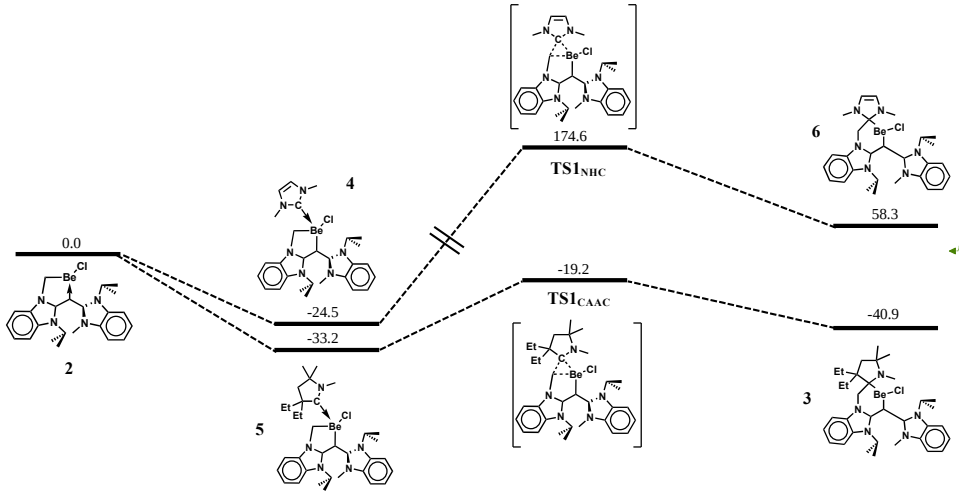

Figure 5. Ring expansion pathway for **2** with ^{Me}NHC and ^{Me}CAAC. Calculated relative free energies (ΔG, kJ mol^{-1}) at the B3LYP-D3(BJ)/def2-TZVPP//B3LYP-D3(BJ)/def2-SVP (SMD, toluene) level of theory.

Consideration of the molecular and electronic structure provides further insight into the observed reactivity. The B3LYP-D3(BJ)/def2-SVP (SMD, toluene) optimized geometries are consistent with the crystal structures, with C1–Be1 bond distances of 1.801 Å (**1**), 1.760 Å (**2**), 1.751 Å (**3**) and 1.865 Å (**4**). The shorter C1–Be1 bond in **2** compared to **1** is reflected in the NBO Wiberg bond index (WBI) values of 0.18 (**1**) and 0.20 (**2**). Quantum theory of atoms in molecules (QTAIM) analysis also supports the stronger interaction in **2**, with the electron density at the C1-Be1 bond critical point (BCP) being greater in **2** (0.073 e/Å^3) compared to **1** (0.069 e/Å^3). The QTAIM charge on the carbone carbon is also higher in **2** (-0.54) than in **1** (-0.50), reflecting a larger contribution from the carbone in **2** that is consistent with the analysis described above.

For compounds **1** and **2** the HOMO is a π-symmetric lone-pair centered on the carbone carbon (Figure 6), which is suggestive of a dative ^{carbone}C–Be bonding interaction. The LUMO of **2** is

Formatted: Indent: First line: 0 cm

situated primarily on the NHC moiety of the CDC with sizable coefficients at the carbene C, which suggests potential for π-accepting behavior on the carbene C, and is consistent with recent experimental observations with CDC.[16] The LUMO of **1** is calculated to be 0.17 eV higher in energy than for **2** (Table 1), making **1** less electrophilic and less reactive towards the carbenes. Indeed, both the electronic structure and the steric repulsion of the bulky $N(SiMe_3)_2$ group opposes the potential for reactivity of **1** with carbenes. Similarly, the lower energy LUMO of ^{Me}CAAC compared to ^{Me}NHC (Table 1) results in the interaction between **2** and ^{Me}CAAC being more favorable, as expected.

(a)

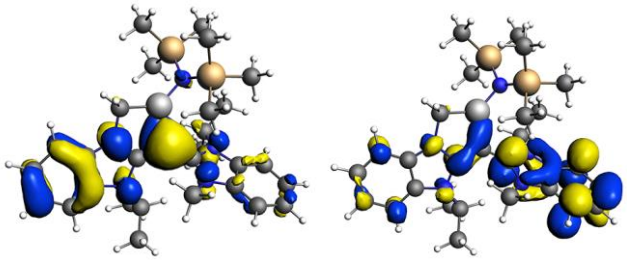

(b)

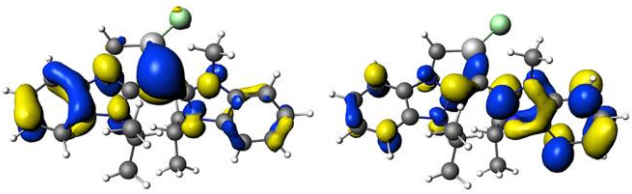

Figure 6. Plots of HOMO and LUMO of **1** (a) and **2** (b).

Formatted: Line spacing: single

Formatted: Line spacing: 1.5 lines

Table 1. B3LYP-D3(BJ)/def2-SVP (toluene) calculated MO energies and HOMO-LUMO gap (eV), and vertical singlet-triplet gap (kcal/mol).

Compound	HOMO	LUMO	H~~OMO~~-L gap~~UMO~~	ΔE_{ST}
NHC^{Me}	-6.07	0.42	6.49	93.1
CAAC^{Me}	-5.35	0.11	5.25	56.6
CDC	-4.32	-0.42	3.91	65.2
1	-4.62	-1.00	3.62	60.3
2	-4.87	-1.17	3.70	47.3
3	-4.09	-1.26	2.83	45.5
~~4~~	~~-4.39~~	~~-0.90~~	~~3.49~~	~~40.3~~
~~5~~	~~-4.37~~	~~-0.95~~	~~3.42~~	~~39.0~~
4	-4.39	-0.90	3.49	40.3
5	-4.37	-0.95	3.42	39.0
6	-4.15	-1.25	2.90	45.9

It is instructive to compare the nature of the carbene adducts, **4** (NHC) and **5** (CAAC), to explore why the RER is observed for **5** but not for **4**. While the HOMO and LUMO energies of both carbene adducts are similar in character, both the HOMO-LUMO gap and ΔE_{ST} are larger in **4**, providing greater electronic stability in **4** compared to **5**. EDA and ETS-NOCV analysis of **4** and **5** highlights the interaction between the carbene and the beryllacycle (Table 2). The bonding interaction in both **4** and **5** is well-described by a dative bonding model, with 63-65% electrostatic character and 36% orbital character. The interaction energy of the carbene, ΔE_{int}, is greater in **4** (NHC), which largely arises from reduced Pauli repulsion (ΔE_{Pauli}). ETS-NOCV analysis indicates that the dominant pairwise orbital interaction $\Delta\rho_1$ arises from σ-donation from the carbene C to the Be atom, as illustrated in Figure 7. Back-donation to the empty pπ orbital of the carbene C atom ($\Delta\rho_2$) is significantly weaker in energy.

Table 2. EDA analysis of carbene adducts **4** and **5**, and transition state structures **TS1** (kcal/mol).

Formatted: Indent: First line: 0 cm, Line spacing: single
Formatted Table
Formatted: Centered, Indent: First line: 0 cm, Line spacing: single
Formatted: Indent: First line: 0 cm, Line spacing: single
Formatted: Indent: First line: 0 cm, Line spacing: single, Tab stops: 1 cm, Decimal aligned
Formatted: Indent: First line: 0 cm, Line spacing: single
Formatted: Indent: First line: 0 cm, Line spacing: single, Tab stops: 1 cm, Decimal aligned
Formatted: Indent: First line: 0 cm, Line spacing: single
Formatted: Indent: First line: 0 cm, Line spacing: single, Tab stops: 1 cm, Decimal aligned
Formatted: Indent: First line: 0 cm, Line spacing: single
Formatted: Indent: First line: 0 cm, Line spacing: single, Tab stops: 1 cm, Decimal aligned
Formatted: Indent: First line: 0 cm, Line spacing: single
Formatted: Indent: First line: 0 cm, Line spacing: single, Tab stops: 1 cm, Decimal aligned
Formatted: Indent: First line: 0 cm, Line spacing: single
Formatted: Indent: First line: 0 cm, Line spacing: single, Tab stops: 1 cm, Decimal aligned
Formatted: Tab stops: 1 cm, Decimal aligned
Formatted: Tab stops: 1 cm, Decimal aligned
Formatted: Indent: First line: 0 cm, Line spacing: single
Formatted: Indent: First line: 0 cm, Line spacing: single, Tab stops: 1 cm, Decimal aligned

transition state structures **TS1** (kcal/mol).

	4 (NHC)	5 (CAAC)	TS1~~a~~-NHC	TS1~~b~~-CAAC
ΔE_{int}	-40.1	-36.2	-35.3	-36.6
ΔE_{Pauli}	94.8	105.7	321.7	275.3
ΔE_{elec} [a]	-86.2 (63.9)	-90.4 (63.7)	-192.5 (53.9)	-172.2 (55.2)
ΔE_{orb} [a]	-48.7 (36.1)	-51.5 (36.3)	-164.4 (46.1)	-139.6 (44.8)
ΔE_1 (σ)[b]	-31.4 (64.6)	-32.8 (63.7)	-131.0 (79.7)	-103.6 (74.2)
ΔE_2 (π)[b]	-3.69 (7.6)	-4.61 (9.0)	-19.9 (12.1)	-21.6 (15.5)

[a] Values in parentheses give the percentage contribution to the attractive interactions, ΔE_{elec} + ΔE_{orb}. [b] Values in parentheses give the percentage contribution to the orbital interaction, ΔE_{orb}.

(a)

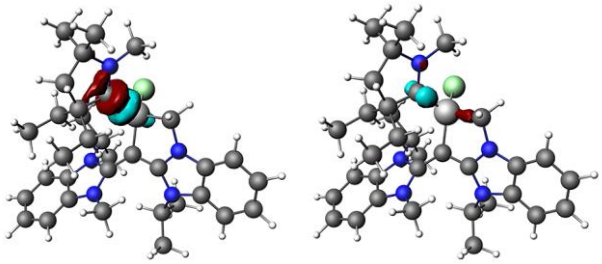

$\Delta\rho_1$, ΔE_1= -32.8 kcal/mol $\Delta\rho_2$, ΔE_2 = -4.61 kcal/mol

(b)

Formatted Table
Formatted: Tab stops: 1 cm, Decimal aligned
Formatted: Tab stops: 1 cm, Decimal aligned
Formatted: Tab stops: 1 cm, Decimal aligned
Formatted: Tab stops: 1 cm, Decimal aligned
Formatted: Tab stops: 1 cm, Decimal aligned
Formatted: Tab stops: 1 cm, Decimal aligned

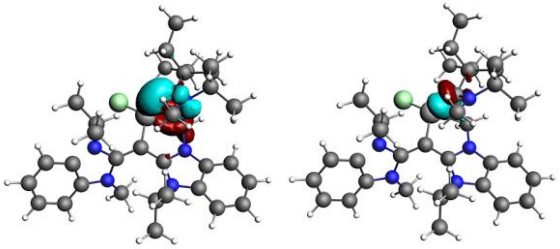

$\Delta\rho_1$, ΔE_1 = -103.6 kcal/mol $\Delta\rho_2$, ΔE_2 = -21.6 kcal/mol

Figure 7. Plots of the deformation densities of the interactions for the pair-wise orbital interactions of the two strongest orbital interactions with the associated interaction energies for (a) compound **5** (interaction between ^{Me}CAAC and **2**), and (b) **TS1**$_{CAAC}$~~b~~. Charge flow is from red to blue.

Formatted: Subscript

Conclusion

We have synthesized a tricoordinate beryllacycle with a terminal chloride (**2**) and explored its reactivity with carbenes. While sIPr coordinated to Be to give a tetrahedral beryllium complex (**4**), ^{Et2}CAAC inserted into a beryllium–carbon bond to form a ring expanded product (**3**). This represents the first example of CAAC promoting a ring expansion reaction. DFT calculations on the transition states for CAAC (14.0 KJ mol^{-1}) and NHC (199.1 kJ mol^{-1}) insertion corroborate the experimental data. In addition, the HOMO-LUMO gap for the NHC adduct **4** was found to be larger than that of a CAAC adduct. These results highlight a new bond activation event involving

beryllium and the first example of a beryllium ring expansion reaction, which contributes to a better understanding of s-block CDC chemistry.

Experimental Section

General Considerations. All manipulations were carried out under an atmosphere of purified argon using standard Schlenk techniques or in a MBRAUN LABmaster glovebox equipped with a −37 °C freezer. All solvents were distilled over sodium/benzophenone or calcium hydride. Glassware was oven-dried at 190 °C overnight. The NMR spectra were recorded at room temperature on a Varian Inova 500 MHz (^{1}H: 500.13 MHz), a Bruker Avance 600 MHz spectrometer (^{1}H: 600.13 MHz, ^{13}C: 150.90 MHz, and ^{9}Be: 84.28 MHz). ^{1}H and ^{13}C chemical shifts are reported in ppm and are referenced using the residual proton and carbon signals of the deuterated solvent (^{1}H; C_6D_6, δ 7.16, ^{13}C; C_6D_6, δ 128.06; ^{1}H; CD_2Cl_2, δ 5.32, ^{13}C; CD_2Cl_2, δ 53.84). All ^{9}Be NMR spectra were referenced to the reported diethyl ether beryllium dichloride $(Et_2O)_2BeCl_2$, δ 1.15.[41] Reference samples were sealed in a capillary tube and placed in the NMR sample tube. IR spectra were recorded on an Agilent Cary 630 FT-IR equipped with a diamond ATR unit in an argon filled glovebox. Single crystal X-ray diffraction data were collected on a Bruker Kappa APEXII Duo diffractometer running the APEX3 software suite using the Mo Kα fine-focus sealed tube (λ = 0.71073 Å) for **2** and **3**, and an Incoatec Microfocus IμS source (Cu K_α, λ = 1.54178 Å) for **4**. The structures were solved and refined using the Bruker SHELXTL Software Package within OLEX2.[51-53] Non-hydrogen atoms were refined anisotropically. Hydrogen atoms were placed in geometrically calculated positions with Uiso = $1.2U_{equiv}$ of the parent atom (Uiso = $1.5U_{equiv}$ for methyl). In compound **2**, the toluene solvent molecule that was located on a crystallographic inversion center was modeled at half-occupancy with a PART-1 command. The crystal data is summarized in Table S1. -Deuterated solvents were purchased from

Acros Organics and Cambridge Isotope Laboratories dried the same way as their protic analogues. Due to the toxicity of the beryllium compounds no combustion analysis was performed. Instead, purity was accessed by ^{1}H, ^{13}C, and ^{9}Be NMR. ***CAUTION!*** Beryllium and its compounds are regarded as HIGHLY TOXIC and carcinogenic. Please adhere to protocols outlined in safety data sheets including using a respirator/mask and working in a well-ventilated fume hood.

Synthesis of compound 2. To a 20 mL scintillation vial (carbodicarbene)(hexamethyldisilazide)beryllacycle (**1**) (558 mg, 1.055 mmol) was stirred in dry toluene (5 mL). A solution of $(Et_2O)_2BeCl_2$ (132 mg, 0.633 mmol) in toluene was added to the stirring solution. After filtration and drying in vacuo, compound **2** was isolated as an air- and moisture-sensitive yellow solid (324 mg, 76% yield). Yellow block-shaped crystals suitable for a single crystal X-Ray diffraction were obtained from a toluene/hexane mixture (5:1) at −37 °C. ^{1}H NMR (500.13 MHz, C_6D_6, 298K) δ 7.07 (m, 1H, Aryl), 7.02 (m, 2H, Aryl), 6.90 (m, 4H, Aryl), 6.52 (m, 1H, Aryl), 5.58 (hept, *J* =7.1 Hz, 1H, N-C*H*$(CH_3)_2$), 3.31 (hept, *J* =7.1 Hz, 1H, N-C*H*$(CH_3)_2$), 2.85 (d, *J* = 15 Hz, 1H, N-C*H*H-Be), 2.78 (d, *J* =15 Hz, 1H, N-C*H*H-Be), 2.59 (s, 3H, N-CH_3), 1.82 (d, *J* =7.1 Hz, 3H, CH(CH_3)$_2$), 1.09 (d, *J*=7.0 Hz, 3H, CH(CH_3)$_2$), 0.99 (d, *J* =7.1 Hz, 3H, CH(CH_3)$_2$), 0.74 (d, *J* =7.0 Hz, 3H, CH(CH_3)$_2$). ^{13}C NMR (151 MHz, C_6D_6, 298K) δ 164.9 (Carbone), 159.1, 137.7, 133.5, 132.9, 130.9, 122.3, 122.1, 121.8, 118.9, 111.3, 110.1, 108.9, 108.1, 49.5, 48.9, 31.8, 31.2, 20.8, 20.5, 19.7, 18.9. ^{9}Be NMR (84.28 MHz, C_6D_6, 298K) δ 18.2. m.p.: decomposed at 174 °C.

Synthesis of compound 3. A suspension of compound **2** (50 mg, 0.124 mmol) in dry toluene (5 mL). A solution of ^{Et2}CAAC (39 mg, 0.124 mmol) in dry toluene (5 mL) was added to the stirring suspension. Upon addition, a yellow product went into solution. The reaction mixture was stirred for 15 minutes. After filtering, drying in vacuo and triturating with hexanes, compound **3** was

obtained as an air- and moisture-sensitive yellow solid (75 mg, 84 % yield). Yellow block-shaped crystals suitable for X-ray diffraction were obtained from a saturated toluene solution at room temperature. ^{1}H NMR (500.13 MHz, C_6D_6, 298K) δ 7.44 (m, 1H, Aryl), 7.29 (m, 4H, Aryl), 7.01 (m, 1H, Aryl), 6.90 (m, 2H, Aryl), 6.80 (m, 1H, Aryl), 6.72 (m, 1H, Aryl), 6.53 (m, 1H, Aryl), 5.73 (hept, *J* = 6.7 Hz, 1H, N–C*H*$(CH_3)_2$), 4.96 (hept, *J* = 6.7 Hz, 1H, Dipp-C*H*$(CH_3)_2$), 4.79 (hept, *J* = 6.4 Hz, 1H, Dipp-C*H*$(CH_3)_2$), 4.55 (d, *J* = 12.6 Hz, 1H, N-CH*H*-CR_2Be), 3.52 (d, *J* = 12.6 Hz, 1H, N-C*H*H-CR_2Be), 3.10 (hept, *J* = 6.7 Hz, 1H, N–C*H*$(CH_3)_2$), 2.98 (d, *J* = 13.1 Hz, 1H, Et_2RC–CH*H*–$CNMe_2$), 2.73 (m, 1H, R_2C(C*H*H–$CH_3)_2$), 2.25 (d, *J* = 13.1 Hz, 1H, Et_2RC–C*H*H–$CNMe_2$), 2.19 (m, 1H, R_2C(C*H*H–$CH_3)_2$), 2.07 (m, 1H, R_2C(C*H*H–$CH_3)_2$), 1.99 (m, 1H, R_2C(C*H*H–$CH_3)_2$), 1.97 (d, , *J* = 6.9 Hz, 3H, CH(C$H_3)_2$), 1.73 (s, 3H, R_2C(C$H_3)_2$), 1.56 (d, *J* = 6.7 Hz, 3H, CH(C$H_3)_2$), 1.52 (d, *J* = 6.7 Hz, 3H, CH(C$H_3)_2$), 1.47 (d, *J* = 6.5 Hz, 3H, CH(C$H_3)_2$), 1.39 (s, 3H, R_2C(C$H_3)_2$), 1.15 (t, *J* = 7.5 Hz, 3H, R_2C(CH_2–C$H_3)_2$), 1.10 (d, *J* = 6.9 Hz, 3H, CH(C$H_3)_2$), 0.98 (d, *J* = 7.0 Hz, 3H, CH(C$H_3)_2$), 0.87 (d, *J* = 6.8 Hz, 3H, CH(C$H_3)_2$), 0.74 (t, *J* = 7.5 Hz, 3H, R_2C(CH_2–C$H_3)_2$), 0.64 (d, *J* = 7.0 Hz, 3H, CH(C$H_3)_2$). ^{13}C NMR (151 MHz, C_6D_6) δ 161.6 (carbone), 157.6, 154.8, 154.4, 141.0, 136.2, 133.1, 131.6, 130.7, 126.0, 124.6, 124.5, 123.1, 122.8, 122.0, 120.0, 112.5, 110.1, 109.4, 108.4, 74.3, 59.9, 52.0, 51.1, 51.0, 49.0, 48.6, 31.5, 31.1, 31.0, 30.4, 28.2, 27.7, 27.4, 27.0, 24.7, 23.7, 22.8, 22.7, 19.6, 19.5, 19.4, 10.2, 9.6. ^{9}Be NMR (84.28 MHz, C_6D_6, 298K) δ 14.0. m.p.: 179-180 °C.

Synthesis of compound 4. Compound **2** (50 mg, 0.124 mmol) was suspended in dry toluene (5 mL) and stirred vigorously. A dry toluene (5 mL) solution of sIPr (22.3 mg, 0.124 mmol) was added to the stirring suspension Upon addition, a yellow product went into solution. After drying the filtrate in vacuo, compound **4** was isolated as an air- and moisture-sensitive yellow solid (68 mg, 94% yield). Yellow crystals suitable for X-ray diffraction were obtained from a toluene

mixture at −37 °C prior to purification. ^{1}H NMR (500.13 MHz, CD_2Cl_2, 298K) δ 7.36 (m, 1H, Aryl), 7.20 (m, 5H, Aryl), 7.04 (m, 2H, Aryl), 6.91 (m, 1H, Aryl), 5.37 (hept, *J* = 6.5 Hz, 1H, N–C*H*$(CH_3)_2$), 5.22 (hept, *J* = 6.8 Hz, 1H, N–C*H*$(CH_3)_2$), 3.78 (hept, *J* = 6.7 Hz, 1H, N–C*H*$(CH_3)_2$), 3.42 (s, 3H, N–CH_3), 2.36 (s, 2H, N-CH_2-Be), 2.18 (s, 6H, C(backbone)–CH_3), 1.64 (d, *J* = 7.0 Hz, 2H, N–CH(CH_3)$_2$), 1.41 (d, *J* = 7.0 Hz, 2H, N–CH(CH_3)$_2$), 1.28 (m, 12H, (sIPr–N–CH(CH_3)$_2$), 1.24 (d, *J* = 7.1 Hz, 2H, N–CH(CH_3)$_2$), 1.20 (d, *J* = 6.4 Hz, 2H, N–CH(CH_3)$_2$). ^{13}C NMR (151 MHz, C_6D_6, 333K) δ 181.5(carbene), 162.8(carbone), 138.8, 135.3, 123.8, 121.5, 121.1, 120.4, 118.5, 109.6, 108.0, 49.1, 35.7, 22.0, 20.6, 20.3, 19.6, 19.2, 9.8. ^{9}Be NMR (84.28 MHz, C_6D_6, 333K) δ 5.3. m.p.: decomposes at 165 °C, further melts at 192-196 °C.

Theoretical Calculations. All calculations were performed using Gaussian 16 revision A.035[54] unless noted. Geometry optimisations were performed using the B3LYP density functional[55] and the def2-SVP[56] basis set inclusive of solvent effects using the polarisable continuum model (IEF-PCM) with Truhlar's SMD model with parameters for toluene (ε = 2.3741).[57] Grimme's D3 dispersion with Becke-Johnson damping was included, labelled D3(BJ).[58] Harmonic vibrational frequencies were computed analytically at the same level of theory in order to characterise the stationary points as minima or transition states (TSs). For all TSs, intrinsic reaction coordinate (IRC) calculations were carried out to ensure connectivity between the local minima along the reaction path. Vibrational frequencies were also utilised to determine corresponding thermochemical data (within the harmonic limit and determined at 1 atm and 298 K). NPA analysis was performed using NBO 6.0 integrated within Gaussian 16.[59] In order to provide more accurate energetics, single-point calculations at the optimised geometries were performed at the B3LYP-D3(BJ) level of theory with a def2-TZVPP basis set, inclusive of solvent effects using the polarisable continuum model (IEF-PCM) with Truhlar's SMD model with parameters for Toluene.

Reported free energies were determined by adding the thermal corrections determined at the B3LYP-D3(BJ)/def2-SVP level of theory to the B3LYP-D3(BJ)/def2-TZVPP solvent-corrected single point energies, which is labelled B3LYP-D3(BJ)/def2-TZVPP//B3LYP-D3(BJ)/def2-SVP (SMD, toluene).

ASSOCIATED CONTENT

Supporting Information. The supporting information is available free of charge on the ACS Publications Website at DOI: XXXXXXXXXX.

CCDC 1917384-1917386 contain the supplementary crystallographic data for this paper. These data can be obtained free of charge from The Cambridge Crystallographic Data Centre, 12 Union Road, Cambridge CB2 1EZ, UK.

AUTHOR INFORMATION

Corresponding Authors

*Email: David.Wilson@latrobe.edu.au, rjg8s@virginia.edu

ORCID

Jacob E. Walley: https://orcid.org/0000-0003-1495-6823

Akachukwu D. Obi: https://orcid.org/0000-0001-7118-7931

Grace Briener: https://orcid.org/0000-0001-5994-934X

Guocang Wang: https://orcid.org/0000-0002-4277-6056

Diane A. Dickie: https://orcid.org/0000-0003-0939-3309

Andrew Molino: https://orcid.org/0000-0002-0954-9054

Jason L. Dutton: https://orcid.org/0000-0002-0361-4441

David J. D. Wilson: https://orcid.org/0000-0002-0007-4486

Robert J. Gilliard, Jr.: https://orcid.org/0000-0002-8830-1064

Notes

The authors declare no competing financial interest.

Acknowledgements

The authors acknowledge the University of Virginia for support of this work. We also thank Xiaofan Jia from the Gunnoe Group at UVA for his assistance with the hydrogenation step of the carbodicarbene ligand synthesis. Generous allocation of computing resources from National Computational Infrastructure (NCI), Intersect and La Trobe University are acknowledged.

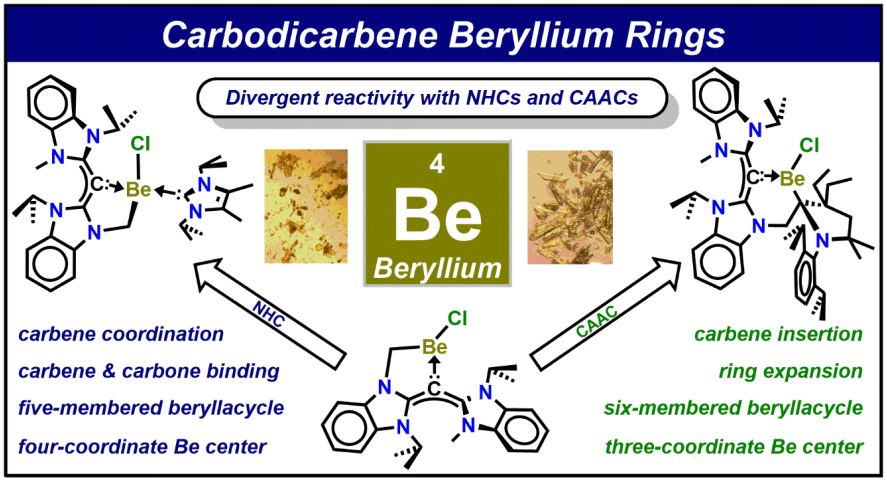

A five-membered carbodicarbene beryllium complex has been synthesized and shows divergent reactivity with N-heterocyclic carbene and cyclic(alkyl)(amino) carbene. Notably, CAAC activates a beryllium-carbon bond and promotes the first ring expansion reaction of a beryllacycle.

References.

1. Arrowsmith, M.; Braunschweig, H.; Celik, M. A.; Dellermann, T.; Dewhurst, R. D.; Ewing, W. C.; Hammond, K.; Kramer, T.; Krummenacher, I.; Mies, J.; Radacki, K.; Schuster, J. K., Neutral zero-valent s-block complexes with strong multiple bonding. *Nat. Chem.* **2016,** *8*, 890.
2. Wang, G.; Freeman, L. A.; Dickie, D. A.; Mokrai, R.; Benkő, Z.; Gilliard Jr., R. J., Isolation of Cyclic(Alkyl)(Amino) Carbene–Bismuthinidene Mediated by a Beryllium(0) Complex. *Chem. - Eur. J.* **2019,** *25*, 4335-4339.
3. Arrowsmith, M.; Hill, M. S.; Kociok-Köhn, G., Activation of N-Heterocyclic Carbenes by {BeH2} and {Be(H)(Me)} Fragments. *Organometallics* **2015,** *34*, 653-662.
4. Arrowsmith, M.; Hill, M. S., Beryllium-Induced C-N Bond Activation and Ring Opening of an N-Heterocyclic Carbene. *Angew. Chem., Int. Ed.* **2012,** *51*, 2098.
5. Buchner, M. R., Recent Contributions to the Coordination Chemistry of Beryllium. *Chem. - Eur. J. 0*, DOI: 10.1002/chem.201901766.
6. Nesterov, V.; Reiter, D.; Bag, P.; Frisch, P.; Holzner, R.; Porzelt, A.; Inoue, S., NHCs in Main Group Chemistry. *Chem. Rev.* **2018,** *118*, 9678-9842.
7. Hopkinson, M. N.; Richter, C.; Schedler, M.; Glorius, F., An overview of N-heterocyclic carbenes. *Nature* **2014,** *510*, 485.

8. Igau, A.; Grutzmacher, H.; Baceiredo, A.; Bertrand, G., Analogous .alpha.,.alpha.'-bis-carbenoid, triply bonded species: synthesis of a stable .lambda.3-phosphino carbene-.lambda.5-phosphaacetylene. *J. Am. Chem. Soc.* **1988,** *110*, 6463-6466.
9. Arduengo, A. J.; Harlow, R. L.; Kline, M., A stable crystalline carbene. *J. Am. Chem. Soc.* **1991,** *113*, 361-363.
10. Lavallo, V.; Canac, Y.; Präsang, C.; Donnadieu, B.; Bertrand, G., Stable Cyclic (Alkyl)(Amino)Carbenes as Rigid or Flexible, Bulky, Electron-Rich Ligands for Transition-Metal Catalysts: A Quaternary Carbon Atom Makes the Difference. *Angew. Chem., Int. Ed.* **2005,** *44*, 5705-5709.
11. Tonner, R.; Frenking, G., C(NHC)2: Divalent Carbon(0) Compounds with N-Heterocyclic Carbene Ligands—Theoretical Evidence for a Class of Molecules with Promising Chemical Properties. *Angew. Chem., Int. Ed.* **2007,** *46*, 8695-8698.
12. Dyker, C. A.; Lavallo, V.; Donnadieu, B.; Bertrand, G., Synthesis of an Extremely Bent Acyclic Allene (A "Carbodicarbene"): A Strong Donor Ligand. *Angew. Chem.* **2008,** *120*, 3250-3253.
13. Chen, W.-C.; Hsu, Y.-C.; Lee, C.-Y.; Yap, G. P. A.; Ong, T.-G., Synthetic Modification of Acyclic Bent Allenes (Carbodicarbenes) and Further Studies on Their Structural Implications and Reactivities. *Organometallics* **2013,** *32*, 2435-2442.
14. Chen, W.-C.; Shen, J.-S.; Jurca, T.; Peng, C.-J.; Lin, Y.-H.; Wang, Y.-P.; Shih, W.-C.; Yap, G. P. A.; Ong, T.-G., Expanding the Ligand Framework Diversity of Carbodicarbenes and Direct Detection of Boron Activation in the Methylation of Amines with CO2. *Angew. Chem., Int. Ed.* **2015,** *54*, 15207-15212.
15. Munz, D., Pushing Electrons—Which Carbene Ligand for Which Application? *Organometallics* **2018,** *37*, 275-289.
16. Chen, W.-C.; Shih, W.-C.; Jurca, T.; Zhao, L.; Andrada, D. M.; Peng, C.-J.; Chang, C.-C.; Liu, S.-k.; Wang, Y.-P.; Wen, Y.-S.; Yap, G. P. A.; Hsu, C.-P.; Frenking, G.; Ong, T.-G., Carbodicarbenes: Unexpected π-Accepting Ability during Reactivity with Small Molecules. *J. Am. Chem. Soc.* **2017,** *139*, 12830-12836.
17. Soleilhavoup, M.; Bertrand, G., Cyclic (Alkyl)(Amino)Carbenes (CAACs): Stable Carbenes on the Rise. *Acc. Chem. Res.* **2015,** *48*, 256-266.
18. Eichhorn, A. F.; Fuchs, S.; Flock, M.; Marder, T. B.; Radius, U., Reversible Oxidative Addition at Carbon. *Angew. Chem., Int. Ed.* **2017,** *56*, 10209-10213.
19. Mohapatra, C.; Samuel, P. P.; Li, B.; Niepötter, B.; Schürmann, C. J.; Herbst-Irmer, R.; Stalke, D.; Maity, B.; Koley, D.; Roesky, H. W., Insertion of Cyclic Alkyl(amino) Carbene into the Si–H Bonds of Hydrochlorosilanes. *Inorg. Chem.* **2016,** *55*, 1953-1955.
20. Wang, T.; Stephan, D. W., Carbene-9-BBN Ring Expansions as a Route to Intramolecular Frustrated Lewis Pairs for CO2 Reduction. *Chem. - Eur. J.* **2014,** *20*, 3036-3039.
21. Frey, G. D.; Masuda, J. D.; Donnadieu, B.; Bertrand, G., Activation of Si□H, B□H, and P□H Bonds at a Single Nonmetal Center. *Angew. Chem., Int. Ed.* **2010,** *49*, 9444-9447.
22. Hill, M. S.; Liptrot, D. J.; Weetman, C., Alkaline earths as main group reagents in molecular catalysis. *Chem. Soc. Rev.* **2016,** *45*, 972-988.
23. Bellemin-Laponnaz, S.; Dagorne, S., Group 1 and 2 and Early Transition Metal Complexes Bearing N-Heterocyclic Carbene Ligands: Coordination Chemistry, Reactivity, and Applications. *Chem. Rev.* **2014,** *114*, 8747-8774.
24. Melaimi, M.; Jazzar, R.; Soleilhavoup, M.; Bertrand, G., Cyclic (Alkyl)(amino)carbenes (CAACs): Recent Developments. *Angew. Chem., Int. Ed.* **2017,** *56*, 10046-10068.

25. Chen, W.-C.; Lee, C.-Y.; Lin, B.-C.; Hsu, Y.-C.; Shen, J.-S.; Hsu, C.-P.; Yap, G. P. A.; Ong, T.-G., The Elusive Three-Coordinate Dicationic Hydrido Boron Complex. *J. Am. Chem. Soc.* **2014,** *136*, 914-917.
26. Đorđević, N.; Ganguly, R.; Petković, M.; Vidović, D., E–H (E = B, Si, C) Bond Activation by Tuning Structural and Electronic Properties of Phosphenium Cations. *Inorg. Chem.* **2017,** *56*, 14671-14681.
27. Đorđević, N.; Ganguly, R.; Petković, M.; Vidović, D., Bis(carbodicarbene)phosphenium trication: the case against hypervalency. *Chem. Commun.* **2016,** *52*, 9789-9792.
28. Petz, W.; Dehnicke, K.; Holzmann, N.; Frenking, G.; Neumüller, B., The Reaction of BeCl2 with Carbodiphosphorane C(PPh3)2; Experimental and Theoretical Studies. *Z. Anorg. Allg. Chem.* **2011,** *637*, 1702-1710.
29. Walley, J. E.; Breiner, G.; Wang, G.; Dickie, D. A.; Molino, A.; Dutton, J. L.; Wilson, D. J. D.; Gilliard, J. R. J., s-Block carbodicarbene chemistry: C(sp3)–H activation and cyclization mediated by a beryllium center. *Chem. Commun.* **2019,** *55*, 1967-1970.
30. Wong, Y. O.; Freeman, L. A.; Agakidou, A. D.; Dickie, D. A.; Webster, C. E.; Gilliard, R. J., Two Carbenes versus One in Magnesium Chemistry: Synthesis of Terminal Dihalide, Dialkyl, and Grignard Reagents. *Organometallics* **2019,** *38*, 688-696.
31. Freeman, L. A.; Walley, J. E.; Obi, A. D.; Wang, G.; Dickie, D. A.; Molino, A.; Wilson, D. J. D.; Gilliard, R. J., Stepwise Reduction at Magnesium and Beryllium: Cooperative Effects of Carbenes with Redox Non-Innocent α-Diimines. *Inorg. Chem.* **2019**, DOI: 10.1021/acs.inorgchem.9b01058.
32. Thiele, K.-H.; Lorenz, V.; Thiele, G.; Zönnchen, P.; Scholz, J., [Be(dad)2]: Synthesis and Structure of a Diazabutadieneberyllium Complex. *Angew. Chem., Int. Ed.* **1994,** *33*, 1372-1373.
33. Liu, S.-F.; Wu, Q.; Schmider, H. L.; Aziz, H.; Hu, N.-X.; Popović, Z.; Wang, S., Syntheses, Structures, and Electroluminescence of New Blue/Green Luminescent Chelate Compounds: Zn(2-py-in)2(THF), BPh2(2-py-in), Be(2-py-in)2, and BPh2(2-py-aza) [2-py-in = 2-(2-pyridyl)indole; 2-py-aza = 2-(2-pyridyl)-7-azaindole]. *J. Am. Chem. Soc.* **2000,** *122*, 3671-3678.
34. Paparo, A.; Jones, C., Beryllium Halide Complexes Incorporating Neutral or Anionic Ligands: Potential Precursors for Beryllium Chemistry. *Chem. Asian J.* **2019,** *14*, 486-490.
35. Bonyhady, S. J.; Jones, C.; Nembenna, S.; Stasch, A.; Edwards, A. J.; McIntyre, G. J., β-Diketiminate-Stabilized Magnesium(I) Dimers and Magnesium(II) Hydride Complexes: Synthesis, Characterization, Adduct Formation, and Reactivity Studies. *Chem. – Eur. J.* **2010,** *16*, 938-955.
36. Arrowsmith, M.; Hill, M. S.; Kociok-Köhn, G.; MacDougall, D. J.; Mahon, M. F.; Mallov, I., Three-Coordinate Beryllium β-Diketiminates: Synthesis and Reduction Chemistry. *Inorg. Chem.* **2012,** *51*, 13408-13418.
37. Arrowsmith, M.; Crimmin, M. R.; Hill, M. S.; Kociok-Köhn, G., Beryllium derivatives of a phenyl-substituted β-diketiminate: a well-defined ring opening reaction of tetrahydrofuran. *Dalton Trans.* **2013,** *42*, 9720-9726.
38. Bayram, M.; Naglav, D.; Wölper, C.; Schulz, S., Syntheses and Structures of Homo- and Heteroleptic Beryllium Complexes Containing N,N′-Chelating Ligands. *Organometallics* **2017,** *36*, 467-473.
39. Niemeyer, M.; Power, P. P., Synthesis, 9Be NMR Spectroscopy, and Structural Characterization of Sterically Encumbered Beryllium Compounds. *Inorg. Chem.* **1997,** *36*, 4688-4696.

40. Perera, T. A.; Reinheimer, E. W.; Hudnall, T. W., Photochemically Switching Diamidocarbene Spin States Leads to Reversible Büchner Ring Expansions. *J. Am. Chem. Soc.* **2017,** *139*, 14807-14814.
41. Nöth, H.; Schlosser, D., The Aminolysis of Beryllium Dichloride with Diisopropylamine and Reactions of Some Aminoberyllium Chlorides. *Eur. J. Inorg. Chem.* **2003,** *2003*, 2245-2254.
42. Bruyere, J. C.; Specklin, D.; Gourlaouen, C.; Lapenta, R.; Veiros, L. F.; Grassi, A.; Milione, S.; Ruhlmann, L.; Boudon, C.; Dagorne, S., Cyclic(Alkyl)(Amino)Carbene (CAAC)-Supported Zn Alkyls: Synthesis, Structure and Reactivity in Hydrosilylation Catalysis. *Chem. - Eur. J.* **2019,** *0*.
43. Paul, U. S. D.; Radius, U., Synthesis and Reactivity of Cyclic (Alkyl)(Amino)Carbene Stabilized Nickel Carbonyl Complexes. *Organometallics* **2017,** *36*, 1398-1407.
44. Schuster, J. K.; Roy, D. K.; Lenczyk, C.; Mies, J.; Braunschweig, H., New Outcomes of Beryllium Chemistry: Lewis Base Adducts for Salt Elimination Reactions. *Inorg. Chem.* **2019,** *58*, 2652-2658.
45. Herrmann, W. A.; Runte, O.; Artus, G., Synthesis and structure of an ionic beryllium-"carbene" complex. *J. Organomet. Chem.* **1995,** *501*, C1-C4.
46. Kovar, R. A.; Morgan, G. L., Beryllium-9 and hydrogen-1 magnetic resonance studies of beryllium compounds in solution. *J. Am. Chem. Soc.* **1970,** *92*, 5067-5072.
47. Han, R.; Parkin, G., [Tris(3-tert-butylpyrazolyl)hydroborato]beryllium hydride: synthesis, structure, and reactivity of a terminal beryllium hydride complex. *Inorg. Chem.* **1992,** *31*, 983-988.
48. Han, R.; Parkin, G., Synthesis, structure, and reactivity of {.eta.3-HB(3-tert-Bupz)3}BeCH3, a terminal beryllium alkyl complex supported by tris(3-tert-butylpyrazolyl)hydroborato ligation. *Inorg. Chem.* **1993,** *32*, 4968-4970.
49. Wilson, D. J. D.; Couchman, S. A.; Dutton, J. L., Are N-Heterocyclic Carbenes "Better" Ligands than Phosphines in Main Group Chemistry? A Theoretical Case Study of Ligand-Stabilized E2 Molecules, L-E-E-L (L = NHC, phosphine; E = C, Si, Ge, Sn, Pb, N, P, As, Sb, Bi). *Inorg. Chem.* **2012,** *51*, 7657-7668.
50. Iversen, K. J.; Wilson, D. J. D.; Dutton, J. L., Effects of the electronic structure of five-membered N-heterocyclic carbenes on insertion of silanes and boranes into the NHC C–N bond. *Dalton Trans.* **2015,** *44*, 3318-3325.
51. Bruker (2012). Saint; SADABS; APEX3. Bruker AXS Inc., Madison, Wisconsin, USA.
52. G. M. Sheldrick, *Acta Cryst*. **2009**, A71, 3.
53. O. V. Dolomanov, L. J. Bourhis, R. J. Gildea, J. A. K. Howard and H. J. Puschmann, *Appl. Cryst*., **2009**, 42, 339.
54. Frisch, M. J.; Trucks, G. W.; Schlegel, H. B.; Scuseria, G. E.; Robb, M. A.; Cheeseman, J. R.; Scalmani, G.; Barone, V.; Petersson, G. A.; Nakatsuji, H.; Li, X.; Caricato, M.; Marenich, A. V.; Bloino, J.; Janesko, B. G.; Gomperts, R.; Mennucci, B.; Hratchian, H. P.; Ortiz, J. V.; Izmaylov, A. F.; Sonnenberg, J. L.; Williams; Ding, F.; Lipparini, F.; Egidi, F.; Goings, J.; Peng, B.; Petrone, A.; Henderson, T.; Ranasinghe, D.; Zakrzewski, V. G.; Gao, J.; Rega, N.; Zheng, G.; Liang, W.; Hada, M.; Ehara, M.; Toyota, K.; Fukuda, R.; Hasegawa, J.; Ishida, M.; Nakajima, T.; Honda, Y.; Kitao, O.; Nakai, H.; Vreven, T.; Throssell, K.; Montgomery Jr., J. A.; Peralta, J. E.; Ogliaro, F.; Bearpark, M. J.; Heyd, J. J.; Brothers, E. N.; Kudin, K. N.; Staroverov, V. N.; Keith, T. A.; Kobayashi, R.; Normand, J.; Raghavachari, K.; Rendell, A. P.; Burant, J. C.; Iyengar, S. S.; Tomasi, J.; Cossi, M.; Millam, J. M.; Klene, M.; Adamo, C.;

Cammi, R.; Ochterski, J. W.; Martin, R. L.; Morokuma, K.; Farkas, O.; Foresman, J. B.; Fox, D. J. *Gaussian 16 Rev. A.03*, Wallingford, CT, 2016.
55. Becke, A. D., Density-functional thermochemistry. III. The role of exact exchange. *J. Chem. Phys.* **1993,** *98* (7), 5648-5652.
56. Weigend, F.; Ahlrichs, R., Balanced basis sets of split valence, triple zeta valence and quadruple zeta valence quality for H to Rn: Design and assessment of accuracy. *Phys. Chem. Chem. Phys.* **2005,** *7* (18), 3297-3305.
57. Marenich, A. V.; Cramer, C. J.; Truhlar, D. G., Universal Solvation Model Based on Solute Electron Density and on a Continuum Model of the Solvent Defined by the Bulk Dielectric Constant and Atomic Surface Tensions. *J. Phys. Chem. B* **2009,** *113* (18), 6378-6396.
58. Grimme, S.; Antony, J.; Ehrlich, S.; Krieg, H., A consistent and accurate ab initio parametrization of density functional dispersion correction (DFT-D) for the 94 elements H-Pu. *J. Chem. Phys.* **2010,** *132* (15), 154104.
59. Glendening, E. D.; Reed, A. E.; Carpenter, J. E.; Weinhold, F. *NBO 6.0.*